

Material Science Image Analysis using Quant-CT in ImageJ

Daniela Ushizima¹, Andrea G. C. Bianchi^{1,2}, Christina DeBianchi¹,
E. Wes Bethel¹

¹ Computational Research Division, Lawrence Berkeley National Lab,
Berkeley, CA, USA,

² Federal University of Ouro Preto, UFOP, Ouro Preto, MG, Brazil.

This document was prepared as an account of work sponsored by the United States Government. While this document is believed to contain correct information, neither the United States Government nor any agency thereof, nor the Regents of the University of California, nor any of their employees, makes any warranty, express or implied, or assumes any legal responsibility for the accuracy, completeness, or usefulness of any information, apparatus, product, or process disclosed, or represents that its use would not infringe privately owned rights. Reference herein to any specific commercial product, process, or service by its trade name, trademark, manufacturer, or otherwise, does not necessarily constitute or imply its endorsement, recommendation, or favoring by the United States Government or any agency thereof, or the Regents of the University of California. The views and opinions of authors expressed herein do not necessarily state or reflect those of the United States Government or any agency thereof or the Regents of the University of California.

This work was partially supported by the Office of Energy Research, U.S. Department of Energy, under Contract Number DE-AC02-05CH11231.

Material Science Image Analysis using Quant-CT in ImageJ

Daniela M. Ushizima^a, Andrea G. C. Bianchi^{a,b}, Christina DeBianchi^a and E. Wes Bethel^a

^aCRD, Lawrence Berkeley National Laboratory, Berkeley-CA 94720, USA

^bPhysics Department, Federal University of Ouro Preto, Ouro Preto-MG, Brazil.

ABSTRACT

We introduce a computational analysis workflow to access properties of solid objects using nondestructive imaging techniques that rely on X-ray imaging. The goal is to process and quantify structures from material science sample cross sections. The algorithms can differentiate the porous media (high density material) from the void (background, low density media) using a Boolean classifier, so that we can extract features, such as volume, surface area, granularity spectrum, porosity, among others. Our workflow, Quant-CT, leverages several algorithms from ImageJ, such as statistical region merging and 3D object counter. It also includes schemes for bilateral filtering that use a 3D kernel, for parallel processing of sub-stacks, and for handling over-segmentation using histogram similarities. The Quant-CT supports fast user interaction, providing the ability for the user to train the algorithm via subsamples to feed its core algorithms with automated parameterization. Quant-CT plugin is currently available for testing by personnel at the Advanced Light Source and Earth Sciences Divisions and Energy Frontier Research Center (EFRC), LBNL, as part of their research on porous materials. The goal is to understand the processes in fluid-rock systems for the geologic sequestration of CO₂, and to develop technology for the safe storage of CO₂ in deep subsurface rock formations. We describe our implementation, and demonstrate our plugin on porous material images. This paper targets end-users, with relevant information for developers to extend its current capabilities.

Keywords: segmentation, material science, porous media, carbon sequestration

1. INTRODUCTION

Computed tomography is the result of image reconstruction based on the linear attenuation coefficient map of a scanned three-dimensional object.¹ This imaging acquisition technique allows the user to probe the interior of solid objects and to explore composition of materials, e.g., the constituency of rock samples. Different from the traditional medical CT scans, microtomography (microCT) is largely used in material science — it presents higher image resolution and it operates at higher X-ray energy levels.

One of the major challenges in microCT analysis is the characterization of samples, which are inherently prone to artifacts, such as streaking, shading, rings, etc., and decision making based on extracted descriptors. As part of a sample characterization, we consider computer vision techniques in order to deal with image enhancement, segmentation, feature extraction, and classification. A fully automatic segmentation scheme for X-ray microCT images still needs to be developed because the available commercial softwares have application to a broader range of images; however, they often require sophisticated customizations to be usable to a particular scientific field. Also, current softwares need to be improved to scale up to the high data throughput of imaging facilities.

Our goal is to provide ImageJ tools for quantitative analysis that can be used, shared throughout the scientific community and easily extended. This article presents the plugin Quant-CT and it describes the analysis workflow tailored to recover the volume fraction from porous materials. Such samples contain areas of void, which corresponds to pore space, and dense materials, which correspond to rock, sediments, fluids, and other materials, hereafter referred as background and foreground, respectively.

This paper leverages some Fiji plugins, such as the bilateral filter, the statistical region merging (SRM), and the mathematical morphology operators; the first is responsible for non-iterative anisotropic smoothing

Further author information: (Send correspondence to D.M.U.)
D.M.U.: E-mail: dushizima@lbl.gov, Telephone: 1 510 486 4061

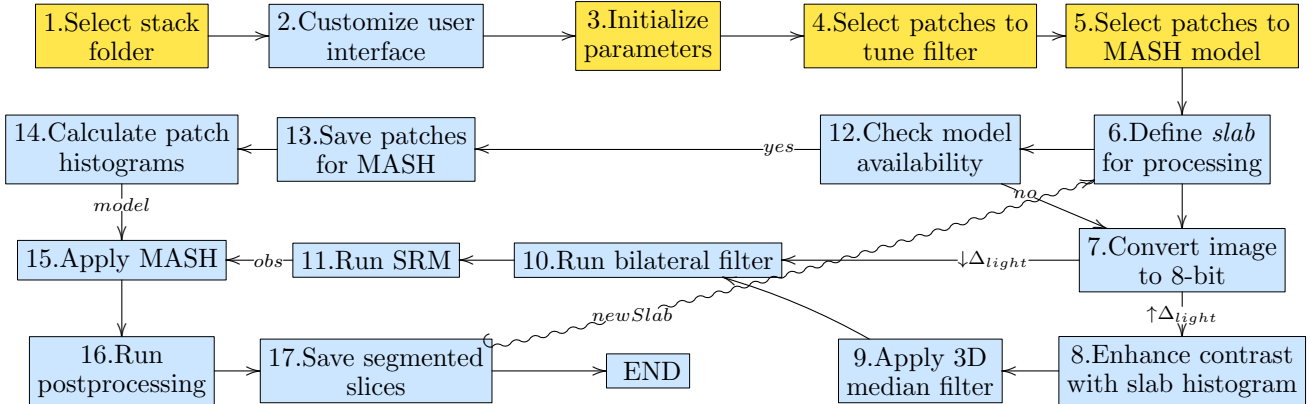


Figure 1: Flow diagram of Quant-CT segmentation workflow: yellow indicates user-interaction event and blue indicates a program action.

to minimize image artifacts; the second calculates volumes of interest, exploiting the intensity similarities of each image segment; and the third eliminates small volumes unlikely to belong to any foreground. The bare combination of the plugins lacked the support for the segmentation of image stacks into void and dense material, therefore, a segmentation workflow was proposed in Ushizima et al.² We built upon this workflow, including a user interface and improvements to deal with SRM over-segmentation. Also, we introduce an algorithm for material assignment based on similarity histograms (MASH) that can tackle over-segmentation even in cases of sharp brightness variations across the image slices. We focus on evaluating our segmentation workflow using receiver operating characteristic (ROC) curves from results obtained by means of the benchmark images available at the Network Generation Comparison Forum (NGCF). This forum provides binary images with geometry that resembles porous media, which we contaminate with increasing amounts of noise to evaluate the accuracy of the Quant-CT segmentation algorithms.

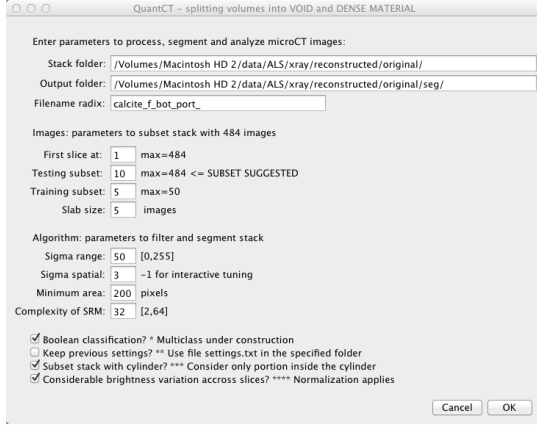
Section 2 explains how the interactive segmentation scheme uses statistics of the patches selected by the user to automatically tune filters and merge the regions detected by the SRM algorithm, to finally separate the image stack into pore and solid volumes using MASH. Section 3 presents the performance of the workflow using the benchmark images under different noise conditions, by means of ROC curves to quantify the accuracy of our method to recover the two sample phases, void and dense matter, under impulsive noise and several levels of additive Gaussian noise. We also illustrate the result of the algorithm in a real dataset. The contribution of this paper is to describe Quant-CT, the current algorithmic updates to deal with brightness variations, inherent in microCT, and to propose an evaluation process using publicly available benchmark images that are representative of porous media datasets.

2. MICROTOMOGRAPHY ANALYSIS WITH QUANT-CT

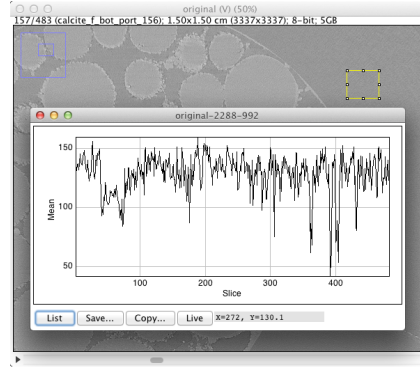
A cumbersome task in imaging materials is to extract information from the very large and high resolution datasets, many times, with billions of pixels per image stack. We can access relevant information from graphical visualizations of the dataset, but in most cases, the hardest task is to provide image segmentation and material characterization. In this realm, our goal is to develop algorithms that combine tuning procedures for image processing and data analysis, which shield the user from implementation details, and deliver measurements from the experimental outcomes. This section presents the plugin Quant-CT and it describes the analysis workflow illustrated in Figure 1, focusing on the pore vs. material segmentation.

2.1 User interface

The user interface of Quant-CT provides control mechanisms for one to choose a volume of interest (VOI) within a porous material, followed by the selection of image subsamples, which then automatically suggest parameters, so that the user can better understand the 3D image datasets. The Quant-CT interface suggests default parameters, but it also offers seamless customization steps to tune parameters by means of image patches (cropped samples



(a) Quant-CT



(b) Brightness variation

Figure 2: (a) Quant-CT interface used to split gray-level image stacks into void and dense material: parameters can be manually set or obtained through the selection of image patches; (b) brightness variation across the 483 slices of a microCT image stack from the subimage determined by the yellow boxed section in the right top corner.

from the original data). Moreover, the user will have a series of prompts with specific parameter options necessary to segment the material sample.

Figure 1 illustrates Quant-CT steps, with yellow boxes indicating the need for user interaction and blue boxes representing automatic program action. The program starts with a request for the user to select an image from a stack folder, through a window with access to the file system (box 1 in Figure 1). Next, a window with basic information regarding the image stack $I(x, y, z)$ is automatically created and it will look similar to Figure 2(a), also box 2. Through this interface, the user is expected to initialize experimental parameters (box 3) which specifies how many data slices to analyze. Another possibility is to use previous parameters (checkbox at the bottom of the user interface), which tells the program that a file named *settings.txt* exists in the current segmentation folder and it can be used to set parameters according to a previous Quant-CT run. Box 4 refers to the user selection of image patches $\hat{I}(k, l, m_i)$, where $|i| = 3$ is used to indicate that the subsample contains 3 adjacent slices from $I(x, y, z)$. Patches \hat{I} are input to the coefficient of variation comparison algorithm that estimates the range of intensity values that characterize a region of interest.² The next user interaction (box 5) consists of selecting new patches corresponding to either the background or the foreground. Also, the coordinates of these subsamples are kept for the later retrieval of the corresponding samples after image enhancement.

Typically, the experimental dataset is partitioned in subsets of slices, which we call *slab* (box 6). The voxel depth of the microCT images were originally 14-bits, however, empirical results show that a conversion to 8-bit (box 7) leads to similar segmentation results. Box 8 represents an optional step (see checkbox at the bottom of Figure 2(a)) that handles image stacks in which the brightness variation (Δ_{light}) across the slices is too large, many times greater than 100 (see Figure 2(b) for an example). If the user marks this checkbox, the program runs the contrast enhancement algorithm using the *slab* histogram, followed by a 3D median filter (box 9) to remove the salt-and-pepper effect often introduced by enhancing the contrast. Box 10 corresponds to the bilateral filter, which uses parameters calculated in the subprogram in box 4. Box 11 indicates that the filtered *slab* is input to the SRM algorithm, and the resulting intensity map is an oversegmented representation of the volume corresponding to the material. Herein, the program splits the binary map into volumes corresponding to void and material by retrieving information from patches for MASH, as shown in box 12. Notice that this step is only calculated for the first program iteration (box 13), and its result is input to the subprogram in box 14. Box 15 corresponds to MASH, which is detailed in Section 2.2. Box 16 refers to the post-processing of a *slab* by: i) applying 3D morphological operators, ii) eliminating objects that are smaller than a minimum area selected by the user at box 3, and iii) removing outliers, i.e. pixels that fall out of a circle with radius 5. A binary version of the images is saved on the output directory (box 17), as specified in box 3.

In addition, the user can choose whether to keep previous parameters or to input new parameters into the user interface, as illustrated in the second checkbox at the bottom of the Figure 2(a). Each time the user customizes the parameters, all the parameter values are recorded. These parameters are sent to the output folder in a *settings.txt* file, together with the segmented data slices, void/dense region samples, and a training subset stack. If the user chooses to run the exact process without modifying previously used values, it is possible to load the file *settings.txt* and load Quant-CT with the same parameters. This option guarantees that the user can make tests with a subset of the whole dataset, and if they are suitable, the user can segment the whole dataset with no need for interaction.

2.2 Image processing and segmentation

In order to achieve an image artifacts attenuation with border preservation, we apply the bilateral filter, an edge-preserving, nonlinear filter, proposed by Tomasi and Maducci,³ to reduce distortions that may come from inherent heterogeneity of the material, light absorption, scattering, positioning of the sample, choice of parameters to the image reconstruction algorithm, among other factors. More details about the performance evaluation of the bilateral filter for synthetic and real microCT images can be found in the study.²

MicroCT images are susceptible to brightness variations across the object slices. The proposed workflow offers contrast enhancement on demand. When this option is selected, Quant-CT automatically runs another nonlinear filter, the 3D median filter, to minimize the salt-and-pepper effect, usually observed when enhancing image contrast based on a linear distribution of the intensity values. The current implementation uses a modified auto-contrast algorithm based on the cumulative histogram of the image in which the mapping function is the result of saturating a fixed percentage of pixels at the lower and upper ends of the target intensity range.⁴ In Quant-CT, we use the same value for both the lower and upper quantiles, with saturation equal to 0.5%.

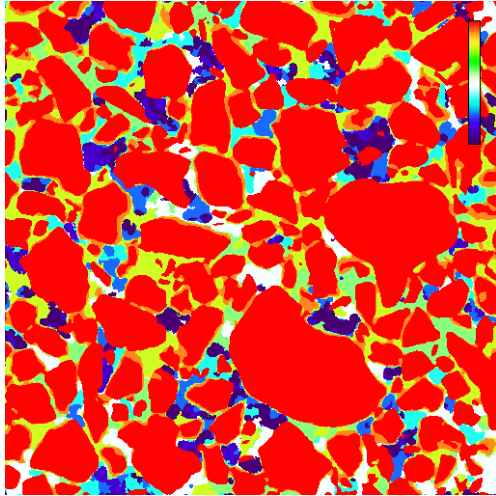
The SRM⁵ algorithm associates a voxel to a region using a similarity criteria, considering both the intensity value and adjacent voxels. The SRM Fiji plugin implementation, by Johannes Schindelin, lies at the core of the Quant-CT segmentation workflow. The goal is to use this fast and robust algorithm to split the microCT images into more homogeneous regions. Our application requires the result of the SRM algorithm to be further agglutinated and to classify regions as belonging to void or material.

Ning et al.⁶ proposed a post-processing technique for agglutination of the mean shift initial segmentation, known as the maximal similarity based region merging (MSRM). Their interactive image segmentation algorithm recovered user-labeled objects from natural scenes in 2D color images by comparing the histogram of different segments in terms of the Bhattacharyya coefficient. This approach was not suitable to microCT because it requires a manual interaction for each slice of the sample, which is not feasible when dealing with image stacks representing sediment information where both the stack size and the number of regions are often very large.

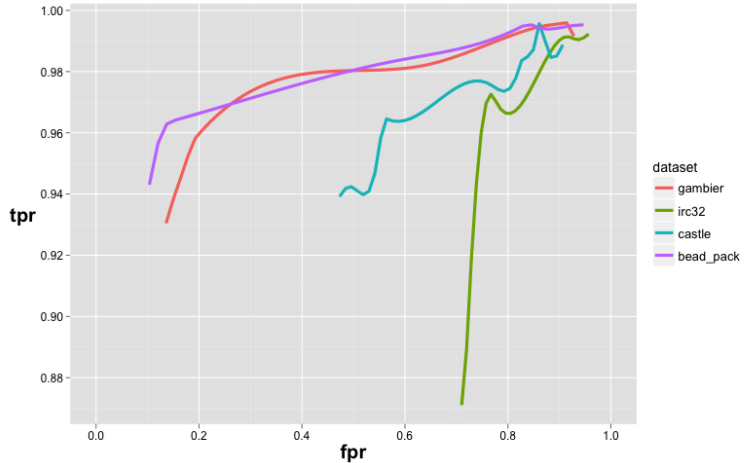
So to go beyond one labeled slice, we designed a new mechanism to generalize user marks to a whole *slab* S using an algorithm for material assignment based on similarity of histograms or MASH. The goal is to calculate a similarity criteria based on the histograms h_1 and h_2 from two *slabs* S_1 and S_2 . Consider the *slabs* as representing the output of SRM (S_r) and the initial user-selected patches that defines the (smaller) *slabs* of foreground and background, S_f and S_b , respectively. First, MASH computes the normalized histogram of the SRM region map that corresponds to a particular *slab*, then it calculates the pointwise product of \hat{h}_r by both the background and foreground normalized histograms, \hat{h}_b and \hat{h}_f , respectively. Next, the algorithm retrieves the argument values that maximizes H_f and H_b , and a cut-off at the medial point between the maxima of H_f and H_b is used to classify regions as void or material. The algorithm is synthesized as follows:

MASH(S_r, S_f, S_b)

- 1 $h_r \leftarrow \text{hist}(S_r); h_f \leftarrow \text{hist}(S_f); h_b \leftarrow \text{hist}(S_b);$
- 2 $\hat{h}_r \leftarrow h_r / \max(h_r); \hat{h}_f \leftarrow h_f / \max(h_f); \hat{h}_b \leftarrow h_b / \max(h_b);$
- 3 $H_b \leftarrow \hat{h}_r * \hat{h}_b; H_f \leftarrow \hat{h}_r * \hat{h}_f;$
- 4 $\max_f \leftarrow \text{argmax} H_f; \max_b \leftarrow \text{argmax} H_b;$
- 5 $\delta \leftarrow |\max_f - \max_b| / 2;$
- 6 **return** (δ)



(a) Segmentation for increasing noise



(b) Algorithm response for increasing noise corruption of datasets

Figure 3: Experimental results using Quant-CT for NGCF 3D image stacks: (a) heatmap of slice 111 from irc32 dataset; (b) ROC curves for the different datasets after noise corruption (salt-and-pepper and additive Gaussian with $\sigma = [0, 300]$).

These algorithms considerably improve the segmentation results, and they are further refined with the 3D morphological opening operations to remove small areas which may appear as byproducts of previous processings.

2.3 Images

One of the main descriptors of the porous material is the pore network⁷ — this is one of the main goals of our research project, and its accuracy depends on Quant-CT segmentation results. Therefore, we selected four representative porous media datasets that well illustrate a reasonable range of porous materials. The data is available at the Network Generation Comparison Forum (NGCF) at http://xct.anu.edu.au/network_comparison (visited on 08/21/12). Each dataset is a cubic segmented image with 512^3 voxels, stored in a raw binary file, with one byte per voxel. The byte ordering is irrelevant, so the files can be read on all CPU types. Voxels are set to 1 to indicate solid phase, and 0 to indicate void phase. The uncompressed files should be exactly 128MB. These benchmark images are made available for the objective comparison of network generation algorithms for 3D tomographic datasets of porous media. Our paper, instead, consider these datasets for segmentation evaluation: we use corrupted versions of these images as input to our segmentation workflow, i.e., noise was added to obtain 20 sets of noisy image stacks for each original binary image stack. These new datasets have decreasing signal-to-noise ratios, with $\text{SNR} = [1.7, 15]$ dB, according to results given by Daniel Sage’s plugin (Biomedical Image Group, EPFL, Switzerland).

3. RESULTS

In order to evaluate the performance of the segmentation workflow, we calculate the ROC curves, which shows the probability of detection (true positives rate or tpr) against the probability of false alarm (false positives rate or fpr) for a range of Gaussian noise values. These curves allow the visualization of the performance of a binary classifier in terms of a configuration parameter that determine fractions of true positive and false positive. Our experiment consist of three parts: (i) first, the binary images are corrupted by salt-and-pepper (“impulsive”) noise, which simulates distortions observed due to the use of contrast enhancement; (ii) the images ($J(x, y, z)$) are corrupted by additive white Gaussian noise ($J(x, y, z) = I(x, y, z) + N(0, \sigma)$), for $\sigma \in [0, 300]$, and finally, (iii) we run Quant-CT taking the several versions of the NGCF datasets as input, which produce different results for the two-class prediction problem. Figure 3(a) illustrates the result of segmentation at $\sigma \in \{0, 110, 132, 138, 146, 150, 180, 200, 300\}$, which corresponds to red, orange, yellow, green, white, cyan, blue, dark blue and purple, respectively — this representation allows a quick accessment of the shape degeneration

(e.g., undesirable component connection, border smoothing) as σ increases, while segmentation is mostly stable for $\sigma \geq 100$ Quant-CT performance for the different datasets is summarized in Figure 3(b), after the simulation of artifacts on porous media using additive white Gaussian noise.^{2,8}

4. CONCLUSIONS AND DISCUSSIONS

We described the plugin Quant-CT and its analysis workflow dedicated to the segmentation and characterization of porous material. This workflow includes traditional and novel algorithms to process and split 3D image stacks into void and pore volume fractions. We defined a rule that splits solid material from void space, and we tested the current approach on images corrupted by impulsive noise and additive Gaussian noise to immitate artifacts that may arise from X-ray interaction with matter and/or image reconstruction issues. Other branches of this research work include devising new features that explain rock geometry, pore network,^{7,9} permeability, and phase distribution of the imaged materials. We expect that this effort will enable the development and deployment of automatic procedures for processing and analyzing microCT data from a wide range of user experiments, and that extensions of Quant-CT will respond to the growing data throughput from light source facilities, as this data continues to rise over the coming years.

ACKNOWLEDGMENTS

We thank Donald J. DePaolo, Center Director of Nanoscale Control of Geologic CO₂, Department of Energy (DOE) Energy Frontier Research Center (EFRC). We also thank J. Ajo-Franklin (Earth Science Division), and A. MacDowell, D. Parkinson (Advanced Light Source, Beamline 8.3.2). This work was supported by the Director, Office of Science, Office of Basic Energy Sciences and Office of Advanced Scientific Computing Research, of the U.S. Department of Energy under Contract No. DE-AC02-05CH11231 through the Scientific Discovery through Advanced Computing (SciDAC) programs Visualization and Analytics Center for Enabling Technologies (VACET). Also, this research was partially supported by the Applied Mathematical Science subprogram of the Office of Energy Research, U.S. Department of Energy, under Contract No. DE-AC03-76SF00098. Andrea G. C. Bianchi was also supported by Capes (BEX 0761/11-7), Capes/Nanobiomed, INEO/CNPq, CNPq (472565/2011-7) and Fapemig (APQ-00802-11).

REFERENCES

- [1] Hsieh, J., [*Computed tomography*], SPIE press (2009).
- [2] Ushizima, D., Parkinson, D., Nico, P., Ajo-Franklin, J., Macdowell, A., Kocar, B., Bethel, W., and Sethian, J., “Statistical segmentation and porosity quantification of 3d x-ray micro-tomography,” *Applications of digital image processing, Proc. of SPIE* **8135**, 1–14 (2011).
- [3] Tomasi, C. and Manduchi, R., “Bilateral filtering for gray and color images,” in [*Proceedings of the Sixth International Conference on Computer Vision*], *ICCV '98*, 839–, IEEE Computer Society, Washington, DC, USA (1998).
- [4] Burger, W. and Burge, M. J., [*Digital Image Processing: an algorithmic introduction using Java*], Springer (2008).
- [5] Nock, R. and Nielsen, F., “Statistical region merging,” *IEEE Transactions on Pattern Analysis and Machine Intelligence* **26**, 1452–1458 (2004).
- [6] Ning, J., Zhang, L., Zhang, D., and Wu, C., “Interactive image segmentation by maximal similarity based region merging,” *Pattern Recognition* **43**, 445–456 (2010).
- [7] Ushizima, D., Morozov, D., Weber, G., Bianchi, A., Sethian, J., and Bethel, W., “Augmented topological descriptors of pore networks for material science,” *IEEE Visualization* (2012).
- [8] Mendrik, A. M., Vonken, E.-J., Rutten, A., Viergever, M. A., and van Ginneken, B., “Noise reduction in computed tomography scans using 3-d anisotropic hybrid diffusion with continuous switch,” *IEEE Trans on Medical Imaging* **28**, 1585 (2009).
- [9] Arns, J. Y., Sheppard, A., Arns, C. H., Knackstedt, M. A., Yelkhovsky, A., and Pinczewski, W. V., “Pore-level validation of representative pore networks obtained from micro-ct images,” in [*International Symposium of the Society of Core Analysts*], 1–12 (2007).